



Forming Features at Screw Rolling of Austenitic Stainless-Steel Billets

M.M. Skripalenko , B.A. Romantsev, S.P. Galkin, L.M. Kaputkina, M.N. Skripalenko, A.V. Danilin, and S.O. Rogachev

(Submitted December 6, 2019; in revised form April 13, 2020; published online June 12, 2020)

Two-high and three-high screw rolling of stainless-steel billets was conducted. Experimental rolling was simulated using DEFORM software. Differences in the way hardness, Cockroft–Latham normalized damage criterion, and rigidity coefficient under stress condition change while two-high and three-high screw rolling were established. Changing of these parameters was investigated in the cross section of the billets at the stationary stage of screw rolling. It was unambiguously shown that, in terms of conducted experiments, there is a tendency for axial fracture while two-high screw rolling, and for ring-shaped fracture while three-high screw rolling. Research has allowed for quantitatively estimating the value of the radius of ring-shaped area for which possible fracture may occur while three-high screw rolling.

Keywords computer simulation, fracture, screw rolling, three-high screw rolling mill, two-high screw rolling mill

1. Introduction

The most widespread techniques of screw rolling are two- and three-high schemes (Ref 1). Two-high screw rolling mills with guiding shoes (Ref 2–4) or with guiding disks (Ref 5) are used for producing hollow shells, whereas three-high screw rolling mills are mostly explored for producing round bars from different materials including steel (Ref 6, 7), titanium (Ref 8), aluminum (Ref 9) alloys, and others. Three-high screw rolling schemes, in some cases, may be applied for piercing to manufacture hollow shells (Ref 10).

Two general types of investigation may be identified among screw rolling processes researches. The first type is associated with studying how materials properties are improved due to fine grain structure obtained by screw rolling (Ref 11), including increasing of strength (Ref 12) and plasticity (Ref 13, 14). The second type is connected with computer simulation application to estimate values of loads and moment of rolls (Ref 15) and stress–strain (SSS) state parameters (Ref 16). Comparing of computer simulation results and experimental data in terms of load and moment on rolls is often done, whereas comparing of computer simulation results and experimental data for SSS is almost absent.

The efficiency of jointly using experimental estimation and computer simulation for prediction of fracture with different screw rolling processes is justified in Ref 17, 18. The way grain structure and hardness distribution differ for stationary and non-

stationary stages of screw rolling of austenitic stainless-steel billet are shown in detail in Ref 19. It is of researchers' interest to identify qualitative and quantitative correlation between hardness and SSS parameters during stationary stages of different screw rolling schemes.

The objective of the present research is to identify forming features during two- and three-high screw rolling of austenitic stainless-steel billets by means of experimental estimation and computer simulation.

2. Materials and Methods

AISI 321 steel billets were rolled in two- and three-high screw rolling mills. Mechanical properties of billets materials were: yield strength—196 MPa, ultimate tensile strength—510 MPa, elongation at break—40%, torsion at break—55%. Billets were 60 mm diameter and 200 mm length. Billets were heated till 1150 °C with 2 h holding. Bar's diameter after two-high rolling was 54 mm, after three-high rolling—52 mm. Two-high rolling was realized in MISIS-130D mill (Mannesmann mill, i.e., with guiding shoes) (Ref 2), three-high screw rolling—in MISIS-100T mill (Ref 1, 11). Rolls' feed angle for MISIS-130D mill was 18°, inclination angle—0°. Roll's feed angle for MISIS-100T mill was 18°, inclination angle—10° (Fig. 1). Rolls rotation frequency was 5.76 rad/s.

One semicircle specimen of 5 mm width was cut out in the middle of the billets after two- and three-high screw rolling in order to study the stationary stage of screw rolling. Cutting of billets was with water cooling, width of cut was 0.1 mm. Slices were done in cross section for all specimens. Measurements of hardness for each slice were done according to Fig. 2(a): horizontal and vertical distance between points was constant and equaled 5 mm. Hardness (HV5) was measured using REICHERTER UH250. Value of hardness for each point of Fig. 2(a) was determined as average of three measurements. Electrolytic etching of slices was done using 10% water solution of C₂H₂O₄ (oxalic acid).

M.M. Skripalenko, B.A. Romantsev, S.P. Galkin, L.M. Kaputkina, M.N. Skripalenko, and A.V. Danilin, Department of Metal Forming, National University of Science and Technology “MISIS”, Leninskiy pr. 4, Moscow, Russia 119049; and S.O. Rogachev, Department of Physical Metallurgy and Physics of Strength, National University of Science and Technology “MISIS”, Leninskiy pr. 4, Moscow, Russia 119049. Contact email: mms@misis.ru.

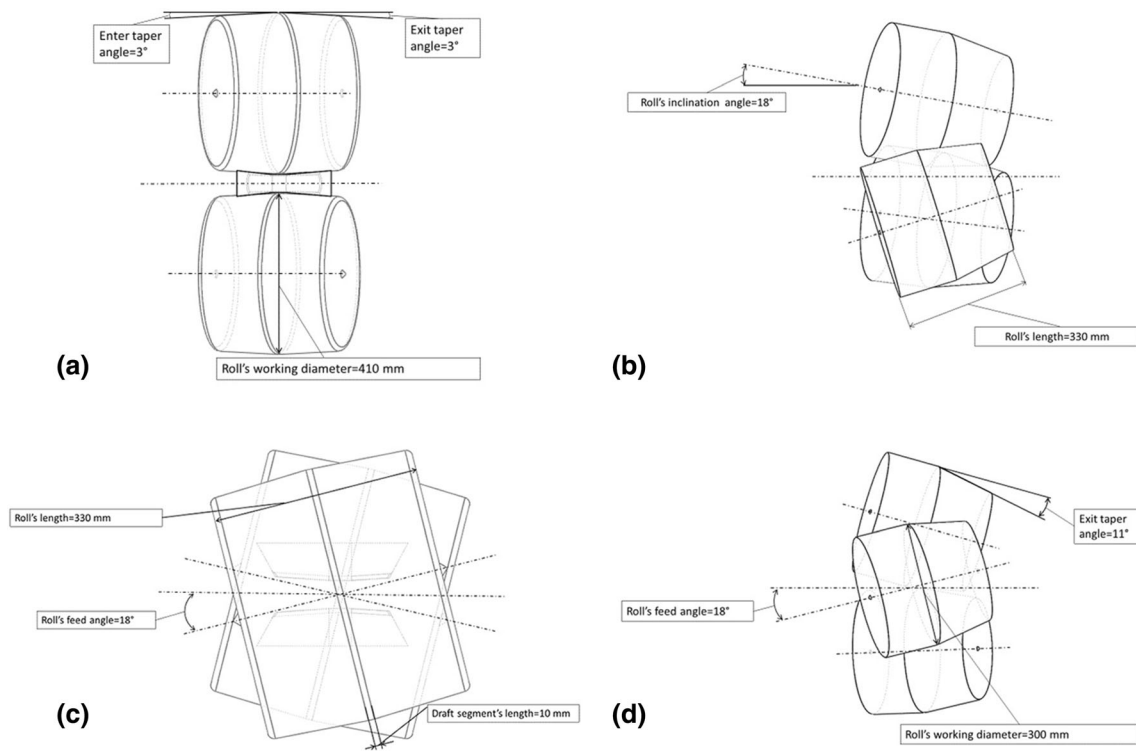


Fig. 1 Positioning of rolls of two-high rolling mill for side (a) and top (c) view and of three-high screw rolling mill for side (b) and top (d) view

Experimental rolling was simulated using DEFORM software. Initially, assemblies (3D models) including rolls, shoes, guides, pusher, and billet were created using SolidWorks. 3D models were saved in .stl format and downloaded into DEFORM pre-processor (Fig. 2). One shoe on Fig. 2(b) and one roll on Fig. 2(c) are not shown for convenience. Specimen were cut out of initial billet and tension tests were done using Gleeble-3800, test data were input in DEFORM materials library and then processed by DEFORM pre-processor. Flow stress data were input for different strain rates and temperatures, curves were initialized by DEFORM inbuilt tool (Fig. 3). All the conditions (initial and boundary) were set in concordance with experimental rolling after 3D models were downloaded in DEFORM pre-processor. Rolls rotation frequency was set 5.76 rad/s, billet's initial temperature was set 1150 °C, environment temperature—20 °C. Simulation was carried out not taking heat transfer between tools and billet into account. The billet had mesh of 100,000 tetrahedral finite elements, friction factor for “roll-billet” couple was set 1 (in Siebel friction law), for “shoe-billet” and “pusher-billet”—0.3, for “guide-billet”—0.12. AISI-321 steel was assigned as billet's material from the DEFORM material library. Flow stress was considered as a function of temperature, strain, and strain rate (Fig. 3).

3. Results and Discussion

To validate the developed numerical model, force parameters from the simulation and experimental studies were

compared. For two-high screw rolling, it was 97 kN (experimental) and 106 kN (simulation), for three-high screw rolling—73 kN (experimental) and 80 kN (simulation). Difference did not exceed 10%.

Hardness variation in cross section of the billets after two- and three-high screw rolling was estimated (Fig. 4). Trend lines on Fig. 4 are governed by third-grade polynomials.

It is shown in Ref 19-21 that hardness correlates with strength, mainly with ultimate strength. It is accepted that the axial zone is the weakest (in terms of strength) at two-high screw rolling (Ref 1, 11, 17, 22), whereas the ring-shaped area of some radiuses is the weakest at three-high screw rolling (Ref 1, 11, 18, 22). According to Fig. 4, minimum hardness values and, hence, strength are in the bar's center at two-high screw rolling and 12-14 mm from the bar's center at three-high screw rolling. SSS parameters were estimated during computer simulation to estimate deformability and identify areas in the rolled bars where fracture is the most probable. Normalized Cockcroft–Latham damage criterion (NCLDC) values were calculated after simulation for points laying on the bar's radius (Fig. 5). NCLDC is calculated by DEFORM according to the formulae:

$$D = \int_0^{\bar{\epsilon}} \frac{\sigma^*}{\bar{\sigma}} d\bar{\epsilon} \quad (\text{Eq 1})$$

where $\bar{\epsilon}$ —accumulated strain, $d\bar{\epsilon}$ —accumulated strain increment, σ^* —maximum principal stress, $\bar{\sigma}$ —stress effective. NCLDC values were calculated for 7 points on the radius of the bar, located in the middle of it, i.e., on the stationary stage of screw rolling (Fig. 5a). There was a 4 mm constant

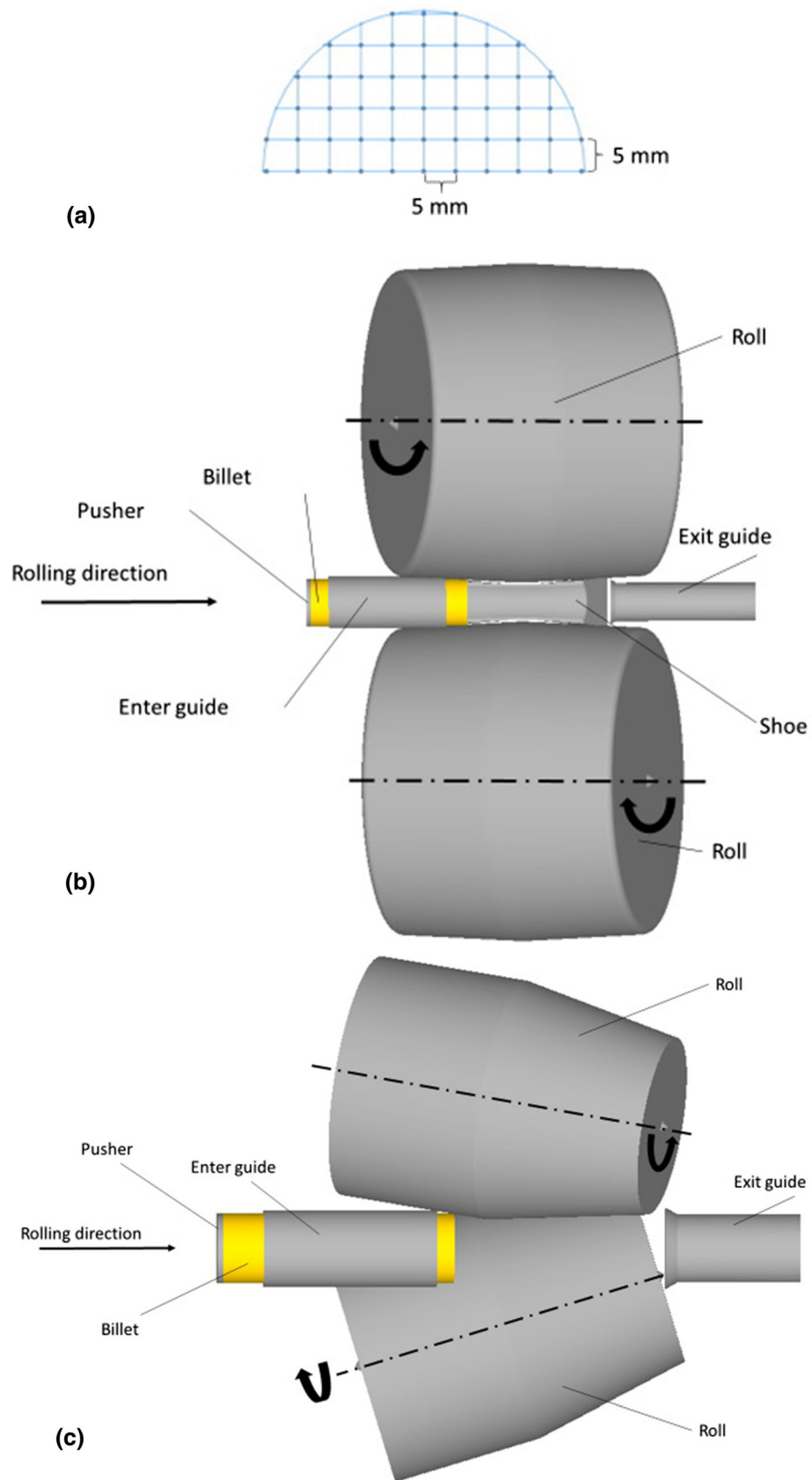


Fig. 2 Scheme of location of points for measuring hardness (a) and 3D models in DEFORM pre-processor for simulation of two-high (b) and three-high (c) screw rolling with arrows showing rolls rotation direction and rolling direction

step between the points. Calculations were done using DEFORM post-processor inbuilt tool («point tracking» command was used), all data were then downloaded into Microsoft Excel. Maximum value through all the screw rolling process was calculated using Microsoft Excel tool for each of the 7 points. Trend lines governed by third-grade polynomials were built to show how NCLDC varies along the radius of the bar while two-high and three-high screw rolling (Fig. 5b).

Computer simulation results (Fig. 5b) confirm data of Fig. 4 for two-high screw rolling: maximum value of NCLDC and, hence, the highest tendency to fracture is in the center of the bar. The highest tendency to fracture at three-high screw rolling, i.e., maximum values of NCLDC, is for the area located 14-15 mm from the bar's center (Fig. 5b). According to Fig. 3, the lowest values of strength and, hence, the highest tendency to fracture are for the area located 12-14 mm from the bar's center (Fig. 4). It is worth noting that the efficiency of using NCLDC at different regimes of two-high screw rolling is shown in Ref 17, whereas results of Ref 18 demonstrates that at three-high radial-shear rolling [three-high screw rolling at high values of feed angle, i.e., more than 18° (Ref 11)] of continuously cast copper billets NCLDC is ineffective. Diameter reduction at two-high and three-high screw rolling, in terms of conducted experiments, is close: 10% for two-high and 12% for three-high screw rolling. At that range of NCLDC values for a three-high scheme is not more than 0.1, whereas for a two-high scheme the range is 0.45 (Fig. 5b). This assumes higher nonuniformity of stresses at two-high screw rolling. The higher range is also for hardness values: 12 HV for two-high screw rolling and 8HV—for three-high screw rolling.

DEFORM simulation also allowed for estimation of changing of rigidity coefficient under stress condition (RCUSC) (Ref 17, 18) along the bar's radius at the stationary stage of screw rolling (Fig. 6). RCUSC is calculated using formulae:

$$\eta = \frac{\sigma_{\text{mean}}}{\bar{\sigma}} \quad (\text{Eq 2})$$

where σ_{mean} —mean stress, $\bar{\sigma}$ —stress effective. The rigidity coefficient under stress condition divided by three is known as stress triaxiality (Ref 23-25). Computer simulation allowed calculation of “mean stress” and “stress effective” by means of DEFORM post-processor for 7 points (Fig. 5a). “Mean stress” and “Stress effective” simulation data were exported from DEFORM post-processor into Microsoft Excel. Mean stress values were divided by stress effective values for each point for each step of the simulation and resulted in RCUSC values. The average value of RCUSC for all the screw rolling process was calculated for each point using Microsoft Excel. Knowing calculated values of RCUSC and distance from the bar's center for each point, trend lines governed by third-grade polynomials were created (Fig. 6). It is known that the higher the RCUSC value, the higher the probability of fracture (Ref 17, 18, 25).

According to Fig. 6, the axial zone has the highest tendency to fracture at two-high screw rolling, and the ring-shaped zone of 13-14 mm radius at three-high screw rolling. Data of Fig. 6 correlate with data represented by Fig. 4. At that for ring-shaped area, the radius (Fig. 6) differs from the experimentally determined one (Fig. 4) by 2 mm. Changes in RCUSC values reveal, as well as changes in NCLDC (Fig. 5b), that higher nonuniformity of stress state at two-high screw rolling is at a

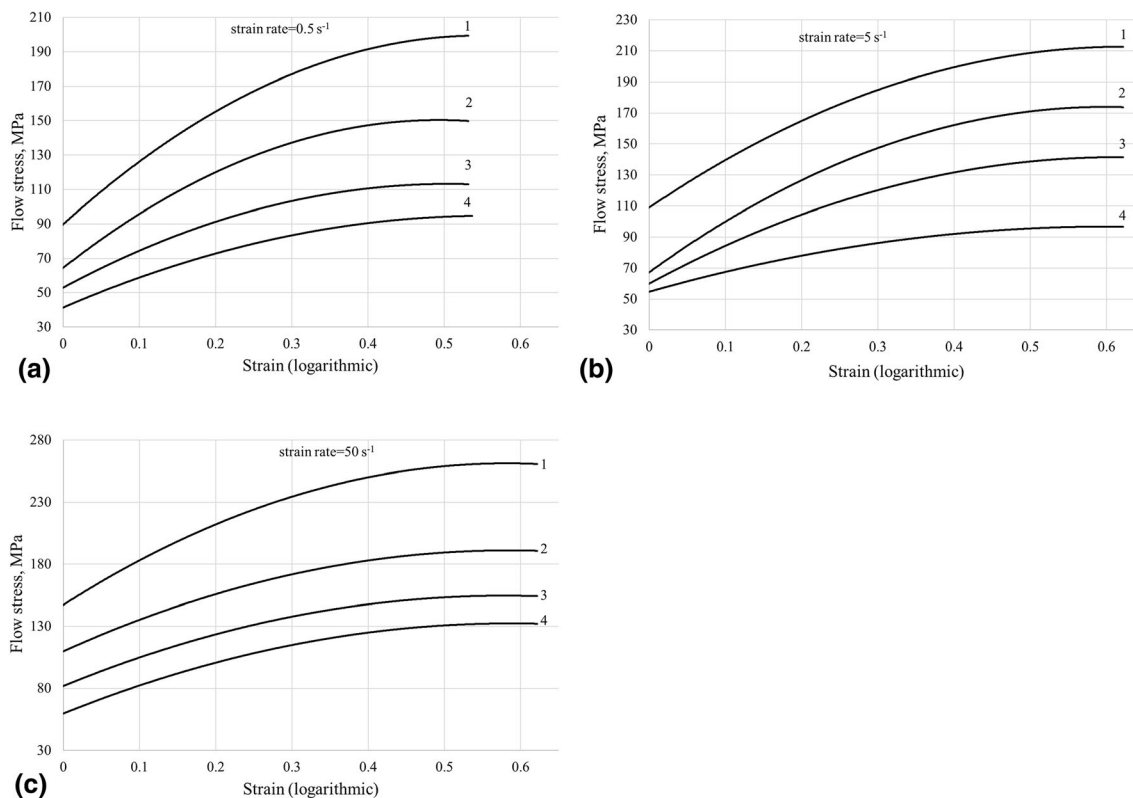


Fig. 3 Variations of the flow stress of AISI-321 steel built on the basis of tensile tests by DEFORM pre-processor for different strain rates and temperatures: 1—900 °C, 2—1000 °C, 3—1100 °C, 4—1200 °C

range of 0.5, whereas at three-high screw rolling the range is not more than 0.2.

It was earlier notified (while discussing Fig. 5 results) that NCLDC criterion works well for two-high screw rolling and can be ineffective when used for predicting possible fracture at three-high screw rolling. The probable reason for such difference in effectiveness is the stress state. According to Fig. 6, RCUSC and, hence, stress triaxiality have negative values in almost the entire cross section of the rolled bar. According to Ref 26, with negative values of stress triaxiality, cracking occurs due to shear fracture, but not due to void nucleation, growth and coalescence. (NCLDC can be used only in this case.) Hence, it seems appropriate to use another

criterion considering shear stress while predicting possible fracture at three-high screw rolling.

4. Conclusions

Two-high and three-high screw rolling of AISI 321 steel billets was carried out. Experimental screw rolling was simulated using DEFORM finite element method software. Researches have allowed estimation of change of hardness, Normalized Cockroft–Latham damage criterion and rigidity

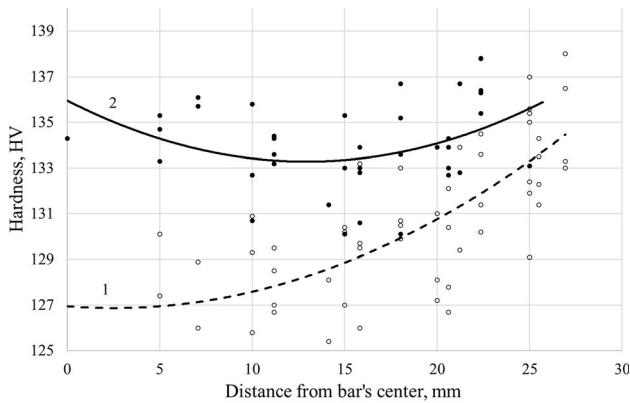


Fig. 4 Change of hardness along the bar's radius at stationary stage after two-high (1) and three-high (2) screw rolling

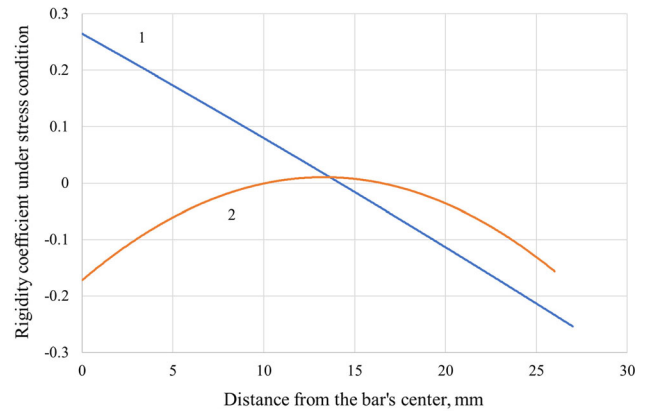
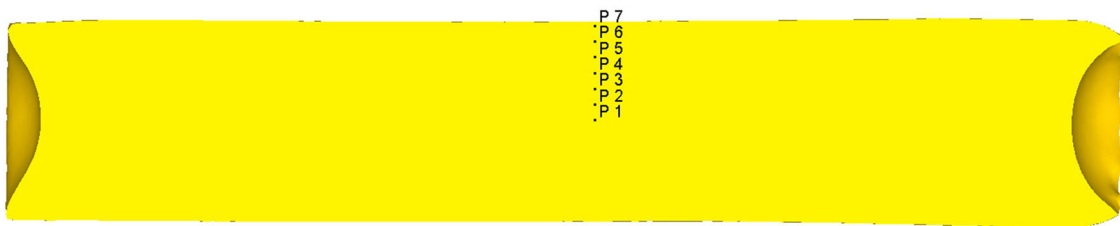
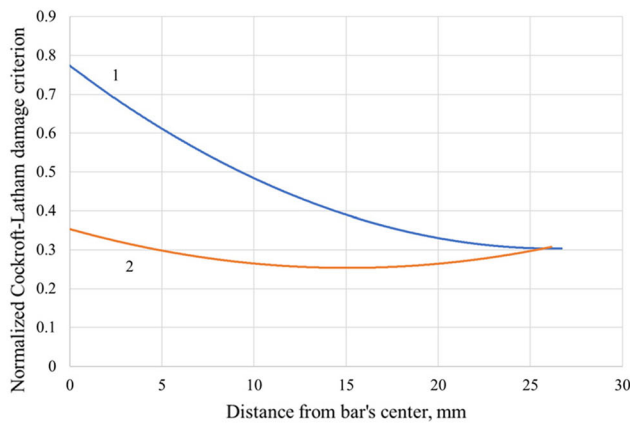


Fig. 6 Change of rigidity coefficient under stress condition along the bar's radius at the stationary stage of two-high (1) and three-high (2) screw rolling



(a)



(b)

Fig. 5 Points for which SSS parameters values were calculated by means of DEFORM computer simulation (a) and variation of normalized Cockroft–Latham damage criterion along the bar's radius (b) at the stationary stage of two-high (1) and three-high (2) screw rolling

coefficient under stress condition at the stationary stage of screw rolling. Change of these parameters demonstrates that at two-high screw rolling, the round bar tends to axial fracture; whereas at three-high screw rolling, there is a tendency to ring-shaped fracture of the rolled bar. At that change of hardness, Normalized Cockcroft–Latham damage criterion and rigidity coefficient under stress condition have monotonous character at two-high screw rolling and with maximum located some distance from the bar's center at three-high screw rolling. Difference between values of these distances (radius) at computer simulation and experimental rolling does not exceed 3 mm. It was shown that using Normalized Cockcroft–Latham damage criterion at three-high screw rolling in terms of realized experiments is effective. Additionally, previous studies using this damage criterion concerning three-high screw rolling of continuously cast copper billets demonstrated its ineffectiveness. In this connection, it seems actual to detect sensitivity of this damage criterion for different materials and at different regimes while three-high screw rolling or to use another fracture criterion considering shear stress while predicting possible fracture at three-high screw rolling.

References

1. B.A. Romantsev, A.V. Goncharuk, N.M. Vavilkin, and S.V. Samusev, *Трубное производство (Pipe Manufacture)*, Izdatelskiy Dom MISiS, 2011 (in Russian)
2. M.M. Skripalenko, V.E. Bazhenov, B.A. Romantsev, M.N. Skripalenko, T.B. Huy, and Yu.A. Gladkov, Mannesmann Piercing of Ingots by Plugs of Different Shapes, *Mater. Sci. Technol.*, 2016, **32**, p 1712–1720
3. V.A. Parfenov, A.E. Shelest, YuD Khesuani, V.S. Yusupov, and M.V. Chepurin, Piercing of Continuous-Cast Billet on Two-Roller Screw Mills with Liners, *Steel Transl.*, 2019, **49**, p 194–197
4. Z. Zhang, D. Liu, Y. Yang, J. Wang, Y. Zheng, and F. Zhang, Microstructure Evolution of Nickel-Based Superalloy with Periodic Thermal Parameters During Rotary Tube Piercing Process, *Int. J. Adv. Manuf. Technol.*, 2019, **104**, p 3991–4006
5. Z. Pater and J. Kazanecki, Complex Numerical Analysis of the Tube Forming Process Using Diescher Mill, *Arch. Metall. Mater.*, 2013, **58**, p 717–724
6. A. Naizabekov, A. Arbut, S. Lezhnev, and E. Panin, The Development and Testing of a New Method of Qualitative Analysis of the Microstructure Quality, For Example of Steel AISI, 321 Subjected to Radial Shear Rolling, *Phys. Scr.*, 2019, **94**, p 1–13
7. L.S. Derevyagina, A.I. Gordienko, and P.O. Kashiro, The Influence of Regimes of Thermomechanical Treatment on the Structural-Phase State, Mechanical Properties, and Fracture Toughness of Low-Alloy Steel API, 5L Grade X52, *Russ. Phys. J.*, 2019, **61**, p 1971–1977
8. D.A. Negodin, S.P. Galkin, E.A. Kharitonov, B.V. Karpov, D.N. Khar'kovskii, I.A. Dubovitskaya, and P.V. Patrin, Testing of the Technology of Radial-Shear Rolling and Predesigning Selection of Rolling Minimills for the Adaptable Production of Titanium Rods with Small Cross Sections Under the Conditions of the "CHMP" JSC, *Metallurgist+*, 2019, **62**(11–12), p 1133–1143
9. N.A. Belov, N.O. Korotkova, T.K. Akopyan, and A.M. Pesin, Phase Composition and Mechanical Properties of Al-1.5%Cu-1.5%Mn-0.35%Zr(Fe,Si) Wire Alloy, *J. Alloys Compd.*, 2019, **782**, p 735–746
10. X. Ding, Y. Shuang, Q. Liu, and C. Zhao, New Rotary Piercing Process for an AZ31 Magnesium Alloy Seamless Tube, *Mater. Sci. Technol.*, 2017, **34**(4), p 408–418
11. S.P. Galkin, Theory and Technology of Stationary Screw Rolling of Billets and Rods Made of Low-Ductility Steels and Alloys. Dissertation, Moscow Institute of Steel and Alloys, Moscow, 1998 (in Russian)
12. S. Dobatkin, S. Galkin, Y. Estrin, V. Serebryany, M. Diez, N. Martynenko, E. Lukyanova, and V. Perezhogin, Grain Refinement, Texture, and Mechanical Properties of a Magnesium Alloy After Radial-Shear Rolling, *J. Alloys Compd.*, 2019, **774**, p 969–979
13. A. Stefanik, P. Szota, S. Mróz, T. Bajor, and H. Dyja, Properties of the AZ31 Magnesium Alloy Round Bars Obtained in Different Rolling, *Arch. Metall. Mater.*, 2015, **60**(4), p 3001–3006
14. I.V. Ratochka, I.P. Mishin, O.N. Lykova, E.V. Naydenkin, and N.V. Varlamova, Structural Evolution and Mechanical Properties of a VT22 Titanium Alloy Under High-Temperature Deformation, *Russ. Phys. J.*, 2016, **59**(3), p 397–402
15. Z. Pater, J. Bartnicki, and J. Kazanecki, 3D Finite Element Method (FEM) Analysis of Basic Process Parameters in Rotary Piercing Mill, *Metallurgija*, 2012, **51**(4), p 501–504
16. Z. Pater, Ł. Wójcik, and P. Walczuk, Comparative Analysis of Tube Piercing Processes in the Two-Roll and Three-Roll Mills, *Adv. Sci. Technol. Res. J.*, 2019, **13**(1), p 37–45
17. M.N. Skripalenko, B.A. Romantsev, S.P. Galkin, M.N. Skripalenko, L. M. Kaputkina, and T.B. Huy, Prediction of the Fracture of Metal in the Process of Screw Rolling in a Two-Roll Mill, *Metallurgist+*, 2018, **61**(11–12), p 925–933
18. M.M. Skripalenko, S.P. Galkin, H.J. Sung, B.A. Romantsev, T.B. Huy, L.M. Kaputkina, M.N. Skripalenko, and A.A. Sidorow, Prediction of Potential Fracturing During Radial-Shear Rolling of Continuously Cast Copper Billets by Means of Computer Simulation, *Metallurgist+*, 2019, **62**(9–10), p 849–856
19. M.M. Skripalenko, B.A. Romantsev, L.M. Kaputkina, S.P. Galkin, M. N. Skripalenko, and V.V. Cheverikin, Study of Transient and Steady-State Stages During Two-High and Three-High Screw Rolling of a 12Kh18N10T Steel Workpiece, *Metallurgist+*, 2019, **63**(3–4), p 366–375
20. M.A. Shaposhnikov, Механические испытания металлов (Mechanical testing of metals), Moscow-Leningrad: Gosudarstvennoe nauchno-tekhnicheskoe izdatelstvo mashinostroitel'noy literature, 1951 (in Russian)
21. D. McLean, *Mechanical Properties of Metals*, 1st ed., Wiley, Hoboken, 1962
22. A.N. Nikulin, Винтовая прокатка. Напряжения и деформации (Screw Rolling. Stresses and Strains), Metallurgizdat, 2015 (in Russian)
23. S. Fanini, *Modelling of the Mannesmann Effect in Tube Piercing*. Ph.D. Thesis, University of Padua, 2008
24. Y. Lou, H. Huh, S. Lim, and K. Pack, New Ductile Fracture Criterion for Prediction of Fracture Forming Limit Diagrams of Sheet Metals, *Int. J. Solids Struct.*, 2012, **49**, p 3605–3615
25. A.V. Vlasov, S.A. Stebunov, S.A. Evsiukov, N.V. Biba, and A.A. Shitikov, Конечно-элементное моделирование технологических процессовковки и объёмной штамповки (Finite Element Method Computer Simulation of Technological Processes of Forging and Die Forging), Izdatelstvo MGTU Imeni N.E. Bauman, 2019 (in Russian)
26. Y. Bai and T. Wierzbicki, A New Model of Metal Plasticity and Fracture with Pressure and Lode Dependence, *Int. J. Plast.*, 2008, **24**, p 1071–1096

Publisher's Note Springer Nature remains neutral with regard to jurisdictional claims in published maps and institutional affiliations.